

A novel PV based high voltage gain soft switching DC-DC boost converter

Ingilala Jagadeesh ¹, V. Indragandhi ² *

¹ Research Scholar, Vellore Institute of Technology, Vellore

² Associate Professor, Vellore Institute of Technology, Vellore

*Corresponding author E-mail: indragandhi.v@vit.ac.in

Abstract

The design of high voltage gain DC-DC boost converter is carried out with the addition of the Voltage Multiplier (VM) method. Here the coupled inductor and VM methodologies are proposed to reduce the switching and conduction losses of the Metal Oxide Semiconductor Field Effect Transistor (MOSFET). The Zero Current Switching (ZCS) technique with coupled inductor leakage inductance is used to operate the MOSFET. The leakage inductance is used to decrease the reverse recovery current across the diode. The design procedure of the boost converter and corresponding output waveforms are presented in this paper. Photovoltaic (PV) source converter with coupling inductors soft switching technique has been analyzed and tested in this paper.

Keywords: DC-DC Power Conversion; High Voltage Gain; Soft Switching; Solar PV; Voltage Multipliers.

1. Introduction

In recent days the demand for the electrical power increasing day by day. Many conventional power generation topologies are proposed but they increase the environmental pollution and consumption of fossil fuels [1 - 8]. There are two types of switching topologies 1) Isolated converters 2) Non-isolated converters. The non-isolated DC to DC converters is Buck, Boost, Cuk, Buck-Boost, Sepic etc. [3]. Fig. 1, shows the classification of DC-DC converters. The isolated converters are Fly-back, Forward converters etc. The isolated converters provide safe operation and eliminate the ground leakage current even it is bulky, less efficient and costly [4].

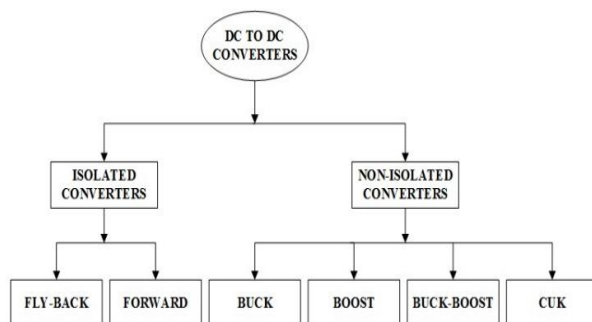


Fig. 1: Classification of DC-DC Converters.

The basic boost converters are used for low and medium power levels. These converters have non-pulsating input current and simple structure. The converter helps in boosting the voltage level of the renewable sources to the level of the grid voltage. The main disadvantages of the basic boost converters are hard switching and high voltage stress on the semiconductor elements. Phase-shifted full-bridge converters used for high step-up gain, it is possible by

increasing the transformer turns ratio. Because of the pulsed input current, the lifetime of photovoltaic array effects greatly [5], [6]. Due to the exhaust of fossil fuels and also the increasing level of pollution renewable sources like solar, wind, hydro, fuel cell, biogas is rapidly used for power generation [9], [10]. The solar energy is intermittent in nature to maintain the stability at load side step up dc-dc converter is required [11]. However, in order to achieve high step-up in these converters turns ratio of isolation transformer need to be increased [12 - 14]. It is preferable to use a coupled inductor in DC to DC converters with the solar panel to achieve high voltage conversion [15].

Full-bridge, fly-back, forward converters used for step-up the voltage levels in solar PV systems [19]. The photovoltaic panel gives DC output by converting the sunlight into electrical energy. The irradiance at morning and evening time is less when compared to the afternoon [20 - 23]. If the solar PV system selected as an energy source the battery stores the excess power during higher irradiation time and supply to the load when the power is required [24 - 29].

For soft switching process, the coupled inductors in addition to the VM techniques are employed in this paper without auxiliary switches. The projected technique introduces soft switching procedure does not depend on the load current and easy to maintain under light load condition. Normally the turn-on commutation of the switch is depending on the ZCS, because of the leakage inductance.

2. Proposed methodology

2.1. PV modelling

PV cell is the basic component of the PV system. The proposed converter consists of two PV modules. The voltage range of one PV module is 12.5 V. The required input voltage of the converter is 24 V. In practice, two PV modules give nearly 24 V. The input

and its relevant output waveforms of the PV system, simulation diagrams are as follows.

2.2. Single diode model

The single diode model is as shown in Fig. 2 provides a tradeoff between complexity and accuracy. By using the diode, current source and resistors a PV generator V-I characteristic can be modeled. Since Thevenin's theorem is not applicable for the nonlinear inherent model. However, the linear model used to represent this nonlinear model with variable parameters.

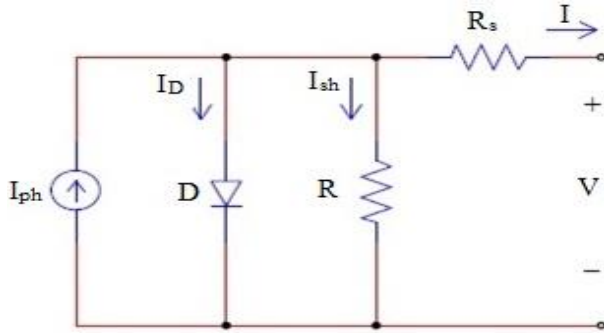


Fig. 2: Single-Diode Model Type PV Generator.

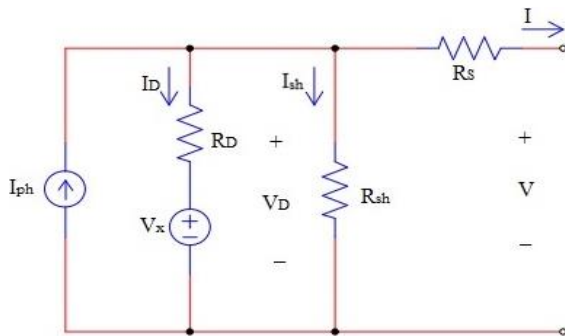


Fig. 3: Single-Diode Model through Linearized Diode.

The solar PV single diode model with a linearized diode is as shown in Fig. 3, where the voltage source V_x represents the diode. The solar PV operation region gives the values of V_x and R_D .

$$V_{pv,th,n} = V_{x,n} + R_{D,n} \cdot \frac{R_{sh} \cdot I_{ph} - V_{x,n}}{R_{sh} + R_{D,n}} \quad (1)$$

$$R_{pv,th,n} = R_s + \frac{R_{sh} \cdot R_{D,n}}{R_{sh} + R_{D,n}} \quad (2)$$

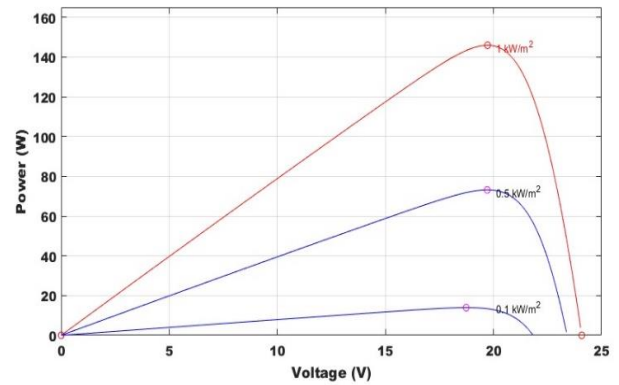


Fig. 4: Power and Voltage characteristics of the PV Panel.

The P - V characteristics of a solar PV module is represented in Fig. 4, due to the stochastic atmospheric conditions the P-V characteristics of a solar PV module are nonlinear. Hence to achieve maximum power from the solar PV it is essential to find the Maximum Power Point Tracking (MPPT) point.

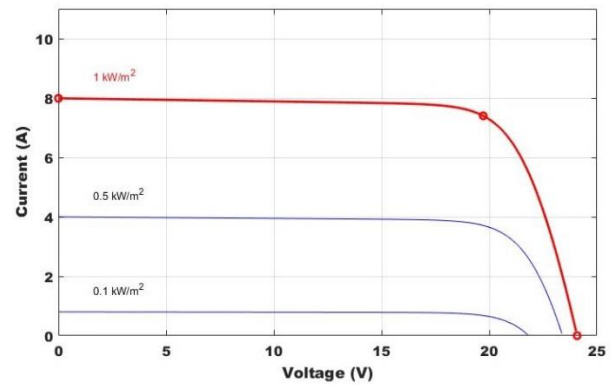


Fig. 5: Current and Voltage Characteristics of the PV Panel.

The V - I characteristics of a solar PV module is represented in Fig. 5, due to the stochastic atmospheric conditions the V - I characteristics of a solar PV module are nonlinear. Hence to achieve maximum power from the solar PV it is essential to find the MPPT point.

3. Converter

The proposed circuit is represented in Fig. 6, which consists of the boost converter and VM. Multiphase converter operation is possible in the proposed converter, for analyzing the operation of the converter through a two-phase circuit is developed. The circuit consists of two power switches S_1 and S_2 , input inductors L_1 and L_2 , the output diodes D_5 and D_6 , and the output filter capacitor C_3 . The capacitors C_1 and C_2 and the diodes D_1 and D_2 compose the VM cell. The high static gain can be achieved by increasing the number of VM cells, which are involved in this converter. The high static gain of the system can be achieved by employing the coupled inductor method in the converter circuit. To avoid the electromagnetic interference of the coupled inductor, the integration must be accomplished. The proposed converter high static gain can be achieved by connecting the coupled inductors L_3 and L_4 in series to the output diodes D_5 and D_6 .

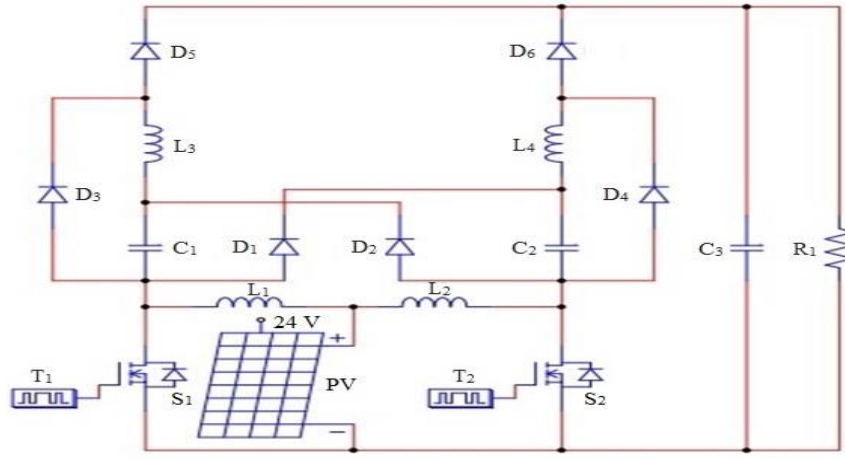


Fig. 6: PV Based ZCS Switch Turn on Using Coupled Inductors and VM Cell Techniques Integrated in the Proposed Converter.

For the switches, S_1 and S_2 the VM circuit works as a non-dissipative snubber and the energy stored in the coupling inductors are transformed into the capacitors C_1 and C_2 . From the output diodes reverse recovery current, the capacitors are received by the leakage inductance energy. Then the effect of leakage inductance energy is removed in the coupled inductors primary and secondary side.

4. Modes of operation

The proposed converter is as shown in Fig. 6, it consists of Continuous Conduction Mode (CCM) and Discontinuous Conduction Mode (DCM) of operations. For Analysis purpose the converter operation is CCM with $D > 5$ in this paper. The converter consists of five modes of symmetric and sequence of operation.

Mode: 1

In this mode, power switches S_1 and S_2 are in on condition. The input DC voltage is applied across the coupling inductors L_1 and L_2 increases linearly and all diodes of the converter are blocked. This stage ends with the power MOSFET S_2 becomes turned off.

$$i_{L2}(t) = i_{L2}(t_0) + \frac{V_{L2}}{L_r} \cdot t \quad (3)$$

$$V_{L1} = V_{L2} = V_i \quad (4)$$

Mode: 2

The power MOSFET S_2 is turned off in this mode. The inductor L_2 dissipates its stored energy through the multiplier diode D_2 , multiplier capacitor C_1 and switch S_1 . By using the output diode D_6 , the L_2 transfer its stored energy to the output side. The maximum switch voltage of the multiplier capacitor V_{S1} is equal to the classical boost converter voltage. The leakage inductance energy is transferred to the capacitor C_1 . The voltage inductance of secondary winding V_{L4} is equal to the product of voltage inductance of the primary inductance and the winding turns ratio. This stage ends with the diode current D_2 becomes zero.

$$V_{S1} = V_{S2} = V_i \cdot \frac{1}{1-D} \quad (5)$$

$$V_{L2} = V_{C1} - V_i = V_i \cdot \frac{1}{1-D} \cdot V_i \quad (6)$$

$$V_{L4} = V_{L2} \cdot n = \left(V_i \cdot \frac{1}{1-D} - V_i \right) \cdot \frac{N_{L4}}{N_{L2}} \quad (7)$$

Mode: 3

In this stage, the diode D_2 is in turn-off condition. The output diode D_6 is used to transfer the energy to the load. This operation is performing until the power MOSFET S_2 becomes turn on.

Mode: 4

In this instant, by using the ZCS commutation the power MOSFET S_2 becomes turned on. When switch F_2 is turned on, the $\frac{di}{dt}$ is limited with the leakage inductance. The current flowing through the diode D_6 decreases linearly and it becomes blocking stage. The problems with the reverse recovery current of the diode are reduced.

Mode: 5

The output diode D_6 becomes turned off in this instant. To transfer the leakage inductance energy to the capacitor C_2 , The clamping diode D_4 act as a free-wheeling diode. The output voltage is equal to the output diode voltage. Static gain can be represented as,

$$V_0 = V_{S2} + V_{C2} + V_{L4} \quad (8)$$

$$V_0 = \left[\left(\frac{V_i}{1-D} \right) + \left(\frac{V_i}{1-D} \right) + \left(\frac{V_i}{1-D} - V_i \right) \cdot n \right] \quad (9)$$

$$\frac{V_0}{V_i} = \frac{D \cdot n + 2}{1-D} \quad (10)$$

The proposed converter static gain increased with the winding turns ratio "n".

Table 1: Comparison between High Voltage Gain Boost Converter

S. NO	Parameters	Coupled inductor or switched capacitor converter [26]	Series/parallel connections of voltage double converter [27]	Coupled inductor switched-capacitor Converter [28]	Proposed converter coupled inductor/ switched-capacitor
1.	Soft-switching method	Active snubber cell	Active snubber cell	Active clamping	Passive snubber cell
2.	Ideal static gain $\frac{V_0}{V_i}$	$\frac{1+2*n}{1-D}$ Turns ratio-n	$\frac{1+n*s}{1-D}$ Turns ratio-ns	$\frac{2+(1+D)*n}{1-D}$ Turns ratio-n	$\frac{D*n+2}{1-D}$ Turns ratio-n
3.	Soft-switching limit	Depends on load	Depends on load	Depends on load	Independent on load
4.	Capacitors at the power circuit	3	3	3	3
5.	Magnetic core	4	4	2	2
6.	Semiconductors at the power circuit	Diodes:4 Active:2	Diodes:4 Active:2	Diodes:4 Active:2	Diodes:6 Active:2



7.	Capacitors at the soft-switching circuit	4	2	2	2
8.	Efficiency in %	$\eta = 90$	$\eta = 94.8$	$\eta = 92$	$\eta = 94.78$

5. Simulation results

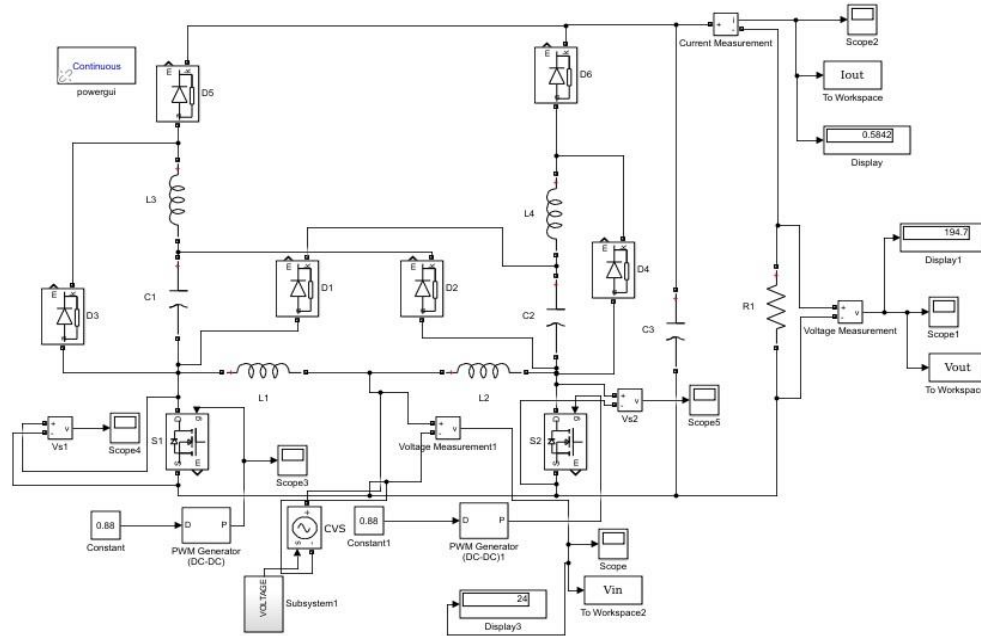


Fig. 7: Simulation Diagram of the Proposed Converter.

The simulation diagram of the PV based ZCS Switch turn on using coupled inductors and VM cell techniques integrated in the proposed converter is shown in Fig. 7, switching frequency $f = 60$ kHz, Input voltage $V_{in} = 24$ V, Duty cycle $D = 0.88$, Inductors $L_1 = L_2 = 100 \mu\text{H}$, Inductors $L_3 = L_4 = 400 \mu\text{H}$, Capacitors $C_1 = C_2 = 3.3 \mu\text{F}$.

5.1. Subsystem

The subsystem for the PV system consists of bypass diode, Insolation to current gain, I_{PV} , V_{PV} , P_{PV} , saturation, product and switch.

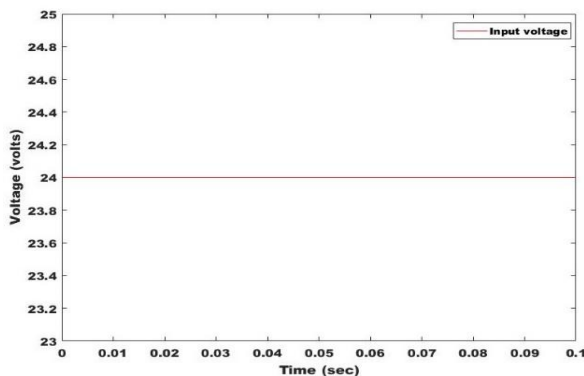


Fig. 8: Proposed System Input Voltage Waveform.

The input voltage for the proposed system supplied by the PV panel which is 24 V. Fig. 8, represents the input voltage 24 V DC supply for the Fig. 6.

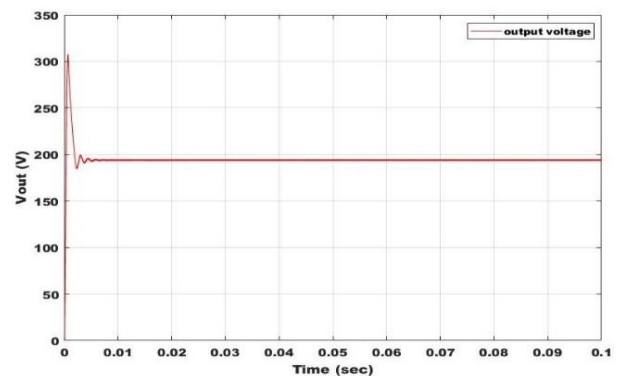


Fig. 9: Proposed System Output Voltage Waveform.

The DC-DC converter output voltage raises from 0 to 307 V with the duration of 0.000668 sec and it reaches the steady-state position at 0.007316 sec. From Fig. 9, it is observed that the settling time for the DC-DC converter voltage is less. Due to the soft switching technique, the voltage stress on the switches reduces. The output voltage of the proposed system is settling at 194.7 V.

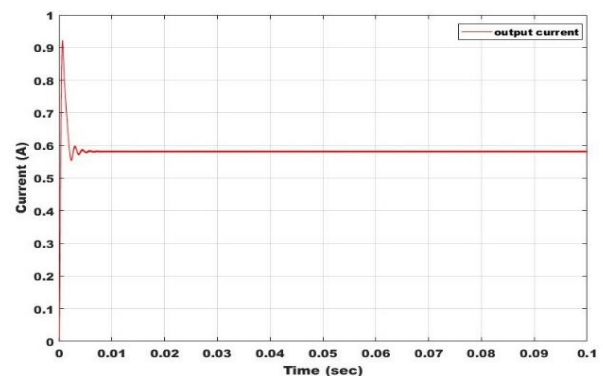


Fig. 10: Proposed System Output Current Waveform.

The DC-DC converter output current raises from 0 to 0.9227 A with the duration of 0.00068 sec and it reach the steady state position at 0.00725 sec. From the Fig. 10, it is observed that the settling time for the DC-DC converter current is less. Due to the soft switching technique the current stress on the switches reduces. The output current of the proposed system is settling at 0.5842 A.

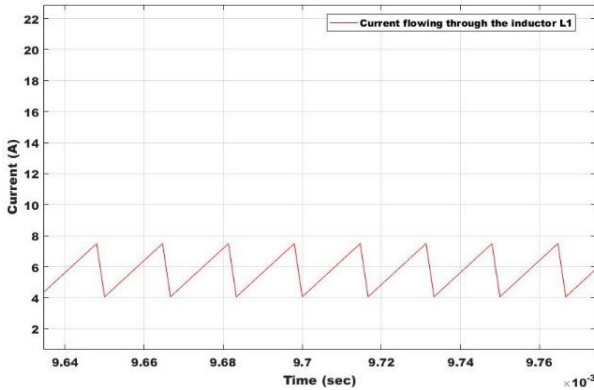


Fig. 11: Current Flowing Through the Inductor L_1 .

The current flowing through the inductor L_1 raises from 0 to 46.86 A with the duration of 0.000348 sec and it reach the steady state position at 0.00795 sec. From the Fig. 11, the current flowing through the inductor L_1 is settling at 4.041 A.

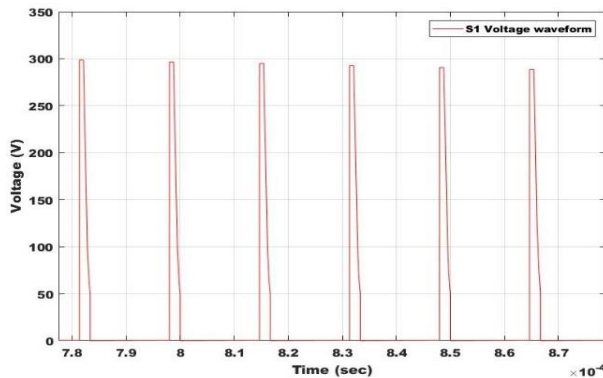


Fig. 12: Voltage Across The MOSFET S_1 .

Fig. 12 shows the voltage across the MOSFET S_1 with the settling time 0.007883 sec.

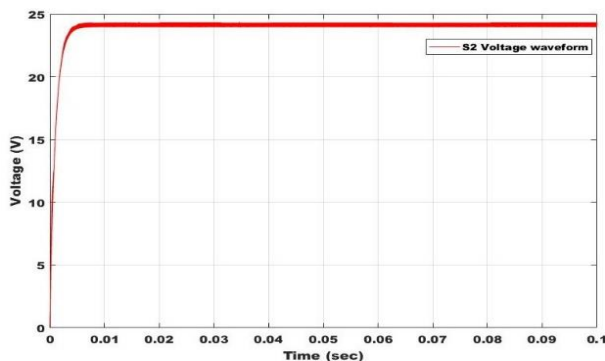


Fig. 13: Voltage Across the MOSFET S_2 .

The voltage across the MOSFET S_2 from 0 to 24 V with the duration of 0.0056 sec and it reach the steady state position at 0.008433 sec. From the Fig. 13, it is observed that the output voltage of the MOSFET S_2 is settling at 24 V.

6. Conclusion

To reduce the voltage stress on the switches in DC-DC converters coupled inductor with VM cells configuration were proposed. The VM clamps the diode voltage and switch voltage. ZCS technique is used for switch turn-on commutation and all diodes reverse recovery current negative effects reduced by the leakage inductance. Low switch voltage maintained by inductor windings and the usage of low R_{DS} on MOSFETs, decrease the conduction losses and increasing the turns ratio of the inductor. The soft commutation is attained without auxiliary switches and not depends on the load current. Compared to classical soft-commutation techniques with controlled auxiliary switches, reduce the cost and complexity of the converter without controlled switches.

References

- [1] M. Das, S. Member, and V. Agarwal, "Design and Analysis of a High-Efficiency DC – DC Converter with Soft Switching Capability for Renewable Energy Applications Requiring High Voltage Gain," *IEEE Transactions on Industrial Electronics*, Vol. 63, no. 5, pp. 2936 – 2944, May 2016. <https://doi.org/10.1109/TIE.2016.2515565>.
- [2] Y. Chen, A. Q. Huang, X. Yu, and S. Member, "A High Step-Up Three-Port DC – DC Converter for Stand-Alone PV / Battery Power Systems," *IEEE Transactions on Power Electronics*, Vol. 28, no. 11, pp. 5049 – 5062, November 2013. <https://doi.org/10.1109/TPEL.2013.2242491>.
- [3] E. Pazouki, S. Member, Y. Sozer, S. Member, and J. A. De, "Fault Diagnosis and Fault-Tolerant Control Operation of Nonisolated DC – DC Converters," *IEEE Transactions on Industry Applications*, Vol. 54, no. 1, pp. 310 – 320, January 2018. <https://doi.org/10.1109/TIA.2017.2751547>.
- [4] N. D. C. D. C. Converters, M. Prudente, L. L. Pfitscher, G. Emmendoerfer, E. F. Romaneli, and R. Gules, "Voltage Multiplier Cells Applied to Non-Isolated DC-DC Converters," *IEEE Transactions on Power Electronics*, Vol. 23, no. 2, pp. 871 – 887, March 2008. <https://doi.org/10.1109/TPEL.2007.915762>.
- [5] F. L. Tofoli, D. D. C. Pereira, and W. J. De Paula, "Survey on non-isolated high-voltage step-up dc – dc topologies based on the boost converter," *IET power Electronics*, Vol. 8, no. 10, pp. 2044 – 2057, July 2015. <https://doi.org/10.1049/iet-pel.2014.0605>.
- [6] W. Li and X. He, "Review of nonisolated high-step-up DC/DC converters in photovoltaic grid-connected applications," *IEEE Transactions on Industrial Electronics*, Vol. 58, no. 4, pp. 1239–1250, April 2011. <https://doi.org/10.1109/TIE.2010.2049715>.
- [7] Y. Zhou, W. Huang, P. Zhao, and J. Zhao, "Coupled-inductor single-stage boost inverter for grid-connected photovoltaic system," *IET Power Electronics*, Vol. 7, no. 2, pp. 259–270, January 2014. <https://doi.org/10.1049/iet-pel.2012.0451>.
- [8] B. R. Lin and J. Y. Dong, "New zero-voltage switching DC-DC converter for renewable energy conversion systems," *IET Power Electronics*, Vol. 5, no. 4, pp. 393, April 2012. <https://doi.org/10.1049/iet-pel.2011.0002>.
- [9] Ram, H., Restrepo, C., Konjedic, T., Calvente, J., Romero, A., Baier, C. R., "An Efficiency Comparison of Fuel-Cell Hybrid Systems Based on the Versatile Buck – Boost Converter," *IEEE Transactions on Power Electronics*, Vol. 33, no.2, pp. 1237–1246, February 2018. <https://doi.org/10.1109/TPEL.2017.2678160>.
- [10] X. Hu, J. Wang, L. Li, and Y. Li, "A Three-Winding Coupled-Inductor DC – DC Converter Topology with High Voltage Gain and Reduced Switch Stress," *IEEE Transactions on Power Electronics*, Vol. 33, no. 2, pp. 1453–1462, February 2018. <https://doi.org/10.1109/TPEL.2017.2689806>.
- [11] Y. Zhang, L. Zhou, M. Sumner, S. Member, and P. Wang, "Single-Switch, Wide Voltage-Gain Range, Boost, DC-DC Converter for Fuel Cell Vehicles", *IEEE Transactions on Vehicular Technology*, Vol. 67, no. 1, pp. 134–145, January 2018. <https://doi.org/10.1109/TVT.2017.2772087>.
- [12] A. R. Gautam, K. Gourav, J. M. Guerrero, and D. M. Fulwani, "Ripple Mitigation with Improved Line-Load Transients Response in a Two-Stage DC-DC-AC Converter: Adaptive SMC Approach," *IEEE Transactions on Industrial Electronics*, Vol. 65, no. 4, pp. 3125–3135, April 2018. <https://doi.org/10.1109/TIE.2017.2752125>.
- [13] B. Gu, J. Dominic, B. Chen, and S. Member, "Hybrid Transformer ZVS / ZCS DC – DC Converter with Optimized Magnetics and Improved Power Devices Utilization for Photovoltaic Module Appli-

- cations," *IEEE Transactions on Power Electronics*, Vol. 30, no. 4, pp. 2127–2136, April 2015. <https://doi.org/10.1109/TPEL.2014.2328337>.
- [14] N. Molavi, H. Farzanehfard, and E. Adib, "Soft-switched non-isolated high step-up DC-DC converter with reduced voltage stress," *IET Power Electronics*, Vol. 9, no. 8, pp. 1711–1718, June 2016. <https://doi.org/10.1049/iet-pel.2015.0870>.
- [15] G. Wu, X. Ruan, and Z. Ye, "High Step-Up DC-DC Converter Based on Switched Capacitor and Coupled Inductor," *IEEE Transactions on Industrial Electronics*, Vol. 65, no. 7, pp. 5572–5579, July 2018. <https://doi.org/10.1109/TIE.2017.2774773>.
- [16] T. Yao, C. Nan, and R. Ayyanar, "New ZVT topology for switched inductor high gain boost," *Conference Proceedings - IEEE Applied Power Electronics Conference and Exposition - APEC*, Vol. 9994, no. c, pp. 2199–2206, March 2017. <https://doi.org/10.1109/APEC.2017.7931004>.
- [17] Yunjie Gu, Wuhua Li, Yi Zhao, Bo Yang, Chushan Li and Xiangning He, "Transformer less Inverter with Virtual DC Bus Concept for Cost-Effective Grid-Connected PV Power Systems," *IEEE Transactions on Power Electronics*, Vol. 28, no. 2, pp. 793–805, February 2013. <https://doi.org/10.1109/TPEL.2012.2203612>.
- [18] C. H. Chang, E. C. Chang, and H. L. Cheng, "A high-efficiency solar array simulator implemented by an LLC resonant DC-DC converter," *IEEE Transactions on Power Electronics*, Vol. 28, no. 6, pp. 3039–3046, June 2013. <https://doi.org/10.1109/TPEL.2012.2205273>.
- [19] J. Zeng, W. Qiao, and L. Qu, "An Isolated Three-Port Bidirectional DC - DC Converter for Photovoltaic Systems with Energy Storage," *IEEE transactions on industry applications*, Vol. 51, no. 4, pp. 3493–3503, July 2015. <https://doi.org/10.1109/TIA.2015.2399613>.
- [20] Martin Breus Meier, S. Avelino da Silva jr., Alceu Andre Badin, Eduardo Felix Ribeiro Romanelli, and Roger Gules, "Soft-Switching High Static Gain DC-DC Converter Without Auxiliary Switches," *IEEE Transactions on Industrial Electronics*, Vol. 65, no. 3, pp. 2335 – 2345, March 2018. <https://doi.org/10.1109/TIE.2017.2739684>.
- [21] P. Xuwei, S. Member, A. K. Rathore, and S. Member, "Naturally Commutated and Clamped Doubler Based Solar PV Inverter," *IEEE 23rd International Symposium on Industrial Electronics (ISIE)*, pp. 2631–2636, July 2014.
- [22] M. Maalandish, S. H. Hosseini, S. Ghasemzadeh, E. Babaei, R. Shalchi Alishah, and T. Jalilzadeh, "Six-phase interleaved boost dc/dc converter with high-voltage gain and reduced voltage stress," *IET Power Electronics*, Vol. 10, no. 14, pp. 1904–1914, July 2017. <https://doi.org/10.1049/iet-pel.2016.1029>.
- [23] R. Errouissi, A. Al-Durra, and S. M. Mueen, "A Robust Continuous-Time MPC of a DC-DC Boost Converter Interfaced with a Grid-Connected Photovoltaic System," *IEEE Journal of Photovoltaics*, Vol. 6, no. 6, pp. 1619–1629, November 2016. <https://doi.org/10.1109/JPHOTOV.2016.2598271>.
- [24] J. Gow and C. Manning, "Development of a photovoltaic array model for use in power electronics simulation studies," *IEE Proceedings-Electric Power Applications*, Vol. 146, no. 6, pp. 193–200, March 2002.
- [25] R.-L. Lin and Y.-F. Chen, "Equivalent circuit model of light-emitting diode for system analyses of lighting drivers," *IEEE Industry Applications Society Annual Meeting*, pp. 1–5, October 2009. <https://doi.org/10.1109/IAS.2009.5324876>.
- [26] R. N. A. Leao, S. Aquino, F. L. Tofoli, P. P. Praca, D. S. Oliveira, and L. H. S. C. Barreto, "Soft Switching high-voltage gain DC-DC interleaved boost converter," *IET Power Electronics*, Vol. 8, no. 1, pp. 120–129, December 2014.
- [27] H. Choi, M. Jang, M. Ciobotaru, and V. G. Agelidis, "Performance evaluation of interleaved high gain converter configurations," *IET Power Electronics*, Vol. 9, no. 9, pp. 1852–1861, July 2016. <https://doi.org/10.1049/iet-pel.2015.0644>.
- [28] D. Wang, X. He, and R. Zhao, "ZVT interleaved boost converters with built-in voltage doubler and current auto-balance characteristic," *IEEE Transactions on Power Electronics*, Vol. 23, no. 6, pp. 2847–2854, November 2008. <https://doi.org/10.1109/TPEL.2008.2003985>.
- [29] A. B. Shitole, S. Sathyan, H. M. Suryawanshi, G. G. Talapur, and P. Chaturvedi, "Soft Switched High Voltage Gain Boost Integrated Flyback Converter Interfaced Single-Phase Grid Tied Inverter for SPV Integration," *IEEE Transactions on Industry Applications*, Vol. 54, no. 1, pp. 482–493, January 2018. <https://doi.org/10.1109/TIA.2017.2752679>.